LETTER

doi:10.1038/nature13272

Niche filling slows the diversification of Himalayan songbirds

Trevor D. Price[1], Daniel M. Hooper[1], Caitlyn D. Buchanan[1], Ulf S. Johansson[1,2], D. Thomas Tietze[1,3], Per Alström[4,5], Urban Olsson[6], Mousumi Ghosh-Harihar[7], Farah Ishtiaq[7], Sandeep K. Gupta[7], Jochen Martens[8], Bettina Harr[9], Pratap Singh[7] & Dhananjai Mohan[7]

Speciation generally involves a three-step process—range expansion, range fragmentation and the development of reproductive isolation between spatially separated populations[1,2]. Speciation relies on cycling through these three steps and each may limit the rate at which new species form[1,3]. We estimate phylogenetic relationships among all Himalayan songbirds to ask whether the development of reproductive isolation and ecological competition, both factors that limit range expansions[4], set an ultimate limit on speciation. Based on a phylogeny for all 358 species distributed along the eastern elevational gradient, here we show that body size and shape differences evolved early in the radiation, with the elevational band occupied by a species evolving later. These results are consistent with competition for niche space limiting species accumulation[5]. Even the elevation dimension seems to be approaching ecological saturation, because the closest relatives both inside the assemblage and elsewhere in the Himalayas are on average separated by more than five million years, which is longer than it generally takes for reproductive isolation to be completed[2,3,6]; also, elevational distributions are well explained by resource availability, notably the abundance of arthropods, and not by differences in diversification rates in different elevational zones. Our results imply that speciation rate is ultimately set by niche filling (that is, ecological competition for resources), rather than by the rate of acquisition of reproductive isolation.

Range expansions are a critical step in the speciation cycle: without them, allopatric and parapatric forms would have ranges of ever decreasing size, unlikely to be further fragmented by barriers[7]. The expansion of geographical range by one taxon inevitably brings it into sympatry with related taxa, which requires reproductive isolation between the forms[1,8] and is generally thought to require ecological differences as well[1,9]. In young adaptive radiations reproductive isolation and ecological divergence may be coupled[10,11], with consequent rapid cycling through the speciation cycle[2] (Extended Data Fig. 1). For example, young species of Darwin's ground finches (*Geospiza*) differ in beak and body size and coexist in sympatry by exploiting different-sized seeds. These beak and body size differences contribute to reproductive isolation, because they are used as cues in conspecific mate choice (premating isolation) and because intermediate-sized hybrids are at a disadvantage in some environments (postmating isolation)[11]. As adaptive radiations proceed and environments fill with species, rates of ecological divergence slow[10,12] and concomitantly the rate of evolution of reproductive isolation declines. Evidence from bird hybrid zones on continents implies that species may continue to interbreed even when separated by more than two million years[2,3], preventing mutual range expansions[4] and delaying the speciation cycle[3].

Here, we introduce a method of studying the causes of slowing speciation rates as species accumulate by considering all species in a sympatric continental community. We ask whether limits to range expansions into the community are attributable to an absence of reproductive isolation or to ecological competition, by considering the age and pattern of diversification along different ecological dimensions, and by directly evaluating species distributions through field measurements of resources. To do this, we built a molecular-based phylogeny for all 461 Himalayan songbirds (Fig. 1). The songbirds (or oscines) are one of three suborders in the order Passeriformes, which is one of the 39 bird orders, but this one suborder contains more than 5,000 species, or over 45% of all the world's birds. Worldwide, they reach their maximum diversity in the eastern Himalayas, where about 358 species breed within our 10,000-km^2 study area (Fig. 1). We consider these species to be sympatric because they are within "cruising range" of one another[8]. They occupy a diversity of climates, from near-tropical to near-boreal, their body mass varies >200-fold (4.5 g to 950 g), their shape differences are extreme (for example, among species weighing about 30 g, beak length varies fivefold) and they include specialist nectarivores, frugivores, granivores, insectivores and aerial foragers, that is, they bear the hallmarks of an adaptive radiation. We assume that ecological differences are essential to coexistence. Previous work on one subgroup of similar species, the Old World leaf warblers (Phylloscopidae, 19 Himalayan species[13]), demonstrated the importance of ecological differences, with sympatric species differing along at least one dimension of feeding method, body size and elevation[14,15].

Biogeographical reconstructions relate many of the speciation events that led to the 358 species in our study area to barrier formation outside the Himalayas, including between the Indonesian islands[16] and within China[13]. Thus, the east Himalayan community has been assembled largely by immigration from outside, with ecological differences either generated *in situ*, or before invasion. We emphasize relationships within a group of sympatric species, rather than within the entire songbird clade, for two reasons. First, many of the other species in the songbird clade (for example, Darwin's finches) have originated in response to ecological conditions elsewhere, so including them would require a complex integration of the timing of establishment and patterns of ecological diversification across the world. Second, many closely related allopatric species apparently occupy the same ecological niche in different places. For example, Päckert *et al.*[17] studied 26 sister species pairs which contained at least one species in our study area; they found that in most cases (63%) the other sister was a similar, allopatric, replacement (see also Extended Data Fig. 2). A collection of closely allopatric replacements that occupy the same niche in different places form a superspecies[1]. Phylogenetic relationships among sympatric species thus capture diversification patterns among superspecies and hence lineage splits that can potentially be limited by niche filling (Extended Data Figs 2 and 3).

Previous phylogenetic analyses of two subgroups of Himalayan songbirds, the Old World leaf warblers[14] and separately, the Corvoidea[18] (57 species) found that differences in elevation generally evolved more recently than differences in feeding method and body size. In Fig. 2 we show this to be the case for the entire 358 species assemblage. Consistent with niche filling along the body size and feeding habit dimensions,

[1]Department of Ecology and Evolution, University of Chicago, Chicago, Illinois 60637, USA. [2]Department of Zoology, Swedish Museum of Natural History, 10405 Stockholm, Sweden. [3]Institute of Pharmacy and Molecular Biotechnology, University of Heidelberg, Im Neuenheimer Feld 364, 69120 Heidelberg, Germany. [4]Key Laboratory of Zoological Systematics and Evolution, Institute of Zoology, Chinese Academy of Sciences, 1 Beichen West Road, Chaoyang District, Beijing 100101, China. [5]Swedish Species Information Centre, Swedish University of Agricultural Sciences, Box 7007, 75007 Uppsala, Sweden. [6]Systematics and Biodiversity, Department of Biology and Environmental Sciences, University of Gothenburg, 40530 Gothenburg, Sweden. [7]Wildlife Institute of India, PO Box 18, Chandrabani, Dehradun 248001, India. [8]Institute of Zoology, Johannes Gutenberg University, Mainz 55099, Germany. [9]Max Planck Institute for Evolutionary Biology, August Thienemannstrasse 2, 24306 Plön, Germany.

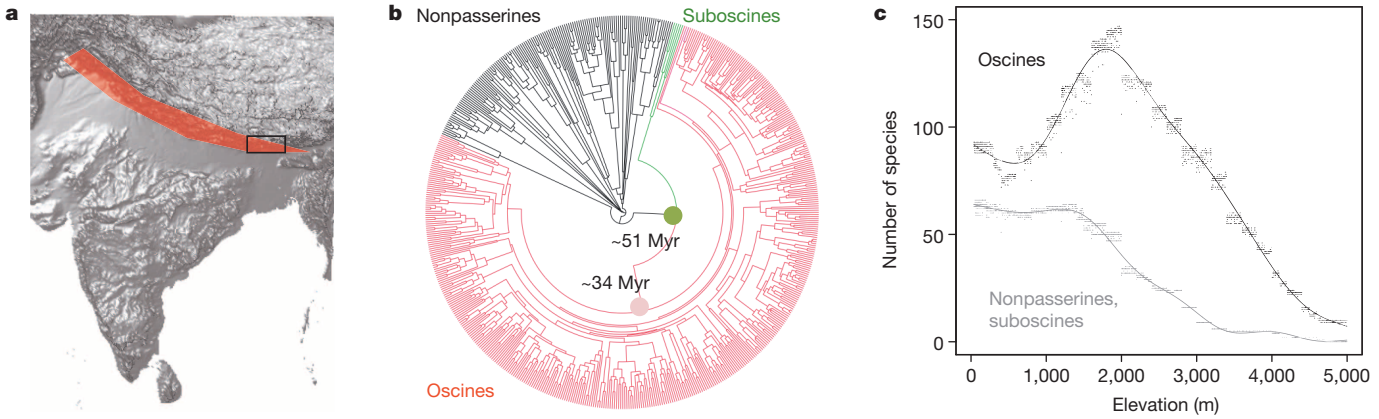

Figure 1 | Phylogeny and species distributions. **a**, Red shading indicates the area covered by the phylogeny and the rectangle denotes the study area. **b**, Estimate of phylogenetic relationships among all Himalayan songbirds (red), suboscines (a second suborder of the Passeriformes, green) and ten orders of nonpasserines (black), computed in BEAST[28] and dated using multiple fossils. 95% confidence limits on dates based on the Bayesian sample are approximately ±3 Myr. **c**, Local abundance of songbirds (oscines) and suboscines + nonpasserines in the study area as assessed by overlapping published range maps with elevational distributions. Lines are nonparametric curve fits. Each point represents the total number of species thought to be breeding in a $0.04^\circ \times 0.04^\circ$ square (about 2 km^2).

rates of diversification in size and shape have significantly slowed towards the present (Extended Data Figs 4 and 5) and clades dating back beyond ten million years (Myr) ago occupy restricted morphological space (for example, Fig. 2b). In contrast, differentiation along the elevation axis has occurred more recently, albeit still many millions of years ago (Fig. 2a, Extended Data Fig. 4). Along with these ecological patterns, lineage splitting in the 358 species phylogeny declines precipitously through time (Fig. 2, Extended Data Table 1). Strikingly, the average time since separation (± the standard error, throughout) of pairs of close relatives ('sister pairs' on the assemblage phylogeny) is estimated as 7.1 Myr ± 0.3, $N = 116$ pairs (97.5% lower bound based on a sample of trees from the a posteriori distribution, 5.6 Myr ± 0.26). These results are consistent with the idea that niche availability limits the establishment of species in the assemblage, with new ecological opportunity[12] along the elevation dimension appearing most recently, perhaps in association with documented climate change (and turnover in the mammalian fossil record) 6 to 10 Myr ago[19].

Although patterns of evolution suggest a dynamic whereby niche-filling slows species accumulation, a failure of species to become established in the assemblage may instead reflect insufficient time to develop reproductive isolation between allopatric forms. However, a strong slowdown in lineage diversification is present even if the phylogeny is truncated at 3 Myr ago (Extended Data Table 1), which is a reasonable upper bound on the time it takes for reproductive isolation to be completed in nature[2,6]; establishment of allopatric forms that are older than this should not be limited by reproductive isolation. Further, 85 Himalayan songbird species are found to the west of our study area. They are separated by an average of 7.5 ± 0.38 Myr from their closest relative in the study area, and 77 of these 85 species breed alongside this close relative somewhere in their western range (overlap of at least 1,500 km^2). Thus, the failure of these 77 species to expand their range into the study area cannot be attributed to incomplete reproductive isolation. We directly evaluated the niche-filling explanation by studying species richness patterns along the elevational gradient. This is the ecological axis associated with the

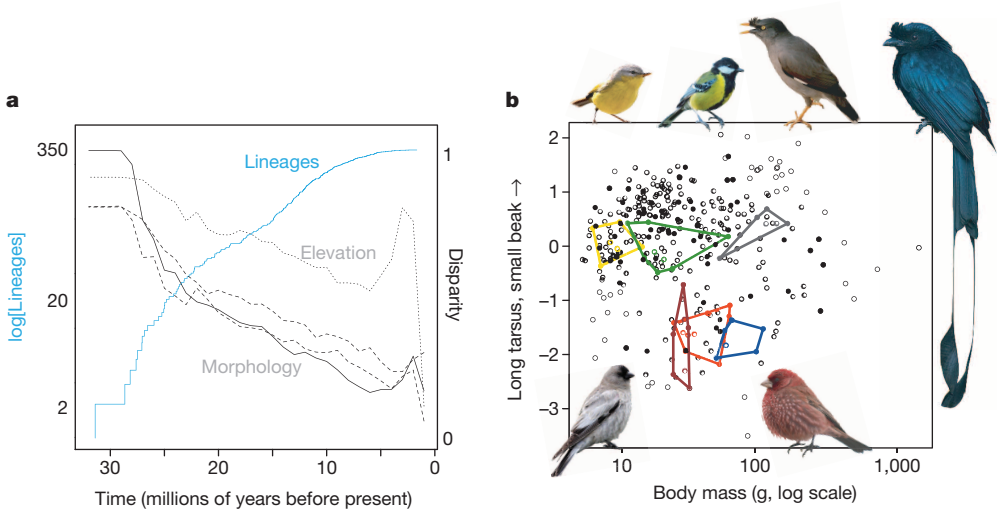

Figure 2 | Morphological evolution. **a**, Number of lineages at a given time slice through the phylogeny (blue solid line) and disparity measures for three morphological traits—mass (solid black line) and two shape measures (dashed black lines)—and elevation (taken as the mid-point of range, dotted black line) for the east Himalayan songbirds. Disparity is a measure of the fraction of the total variance that is within the clades subtended by any timeline[29]. All three disparity measures deviate significantly from a Brownian motion model (Extended Data Figs 4 and 5). **b**, First shape component versus mass. Polygons enclose morphologies for those six lineages at 11.5 Myr ago that subtend at least six species in the study area. One species from each clade is indicated (clockwise from top left *Phylloscopus xanthoschistos, Parus monticolus, Acridotheres fuscus, Dicrurus paradiseus, Carpodacus rubicilla* and *Leucosticte brandti*). The solid points are individual species with no shared relative dating to 11.5 Myr ago. Separate analyses for the major subclades are in Supplementary Table 1.

most recent divergences (Fig. 2) and hence a priori is the dimension most likely to contain additional opportunities for species to differentiate along. Songbirds peak in abundance at an altitude of about 1,800 m in the east Himalayas (Fig. 1). We ask why this should be.

The most popular model that incorporates the slow development of reproductive isolation as a potential explanation for patterns of species richness along elevational gradients considers that each climatic zone independently accumulates species, and different zones accumulate species at different rates[20]. In this model, species and clades present in one zone remain confined to that zone because they are poorly adapted to alternative climates (climatic niche conservatism[20]). In contrast to the predictions of this model, we found that the average age of separation of species in the assemblage declines monotonically with elevation, rather than being lowest in the most species-rich elevational band (Fig. 3a, Extended Data Fig. 6). Further, even at the high elevations, the plot of lineage diversity versus time shows an exceptionally strong slowdown, with close relatives separated by millions of years (Extended Data Fig. 6), suggesting that plenty of time has been available to accumulate additional species in this zone. Finally, climatic niche conservatism along the elevational gradient is weak, with close relatives often found in different zones (see the elevation disparity curve in Fig. 2 and ref. 21). Therefore, there is little support in these data for climatic niche conservatism: newly formed species should be able to transition rapidly between climatic zones in the absence of any other limits.

In models of niche filling, more species are found where resources are either more diverse or more abundant[22]. We tested the resource diversity hypothesis as an explanation for species distribution along the elevational gradient by using morphological diversity as a surrogate[23]. We found that morphological diversity increases from the lowest to intermediate elevations, as may be expected given the increase in species numbers. However, morphological diversity increases still further to the highest elevations, despite the relatively few species at these elevations (Fig. 3b, Extended Data Fig. 7). Exploitation of a relatively high diversity of resources at high elevations has been attributed to a release from competition from the nonpasserines[18], which predominate at lower elevations (Fig. 1c) and may also reflect the presence of additional open country habitats. Whatever the underlying causes, the monotonic increase in the apparent diversity of resources exploited does not match the mid-elevation peak in species richness.

Finally, in a hypothesis of resource abundance a "poor environment supplies too meager a resource base for its would-be rarest species, and they become extinct" (page 56 of ref. 24). To investigate this, over six years, we established eighteen 5-hectare grids in forested habitats at all altitudes across the study area (Extended Data Figs 8 and 9). We censused breeding birds, classified them according to feeding habit, measured

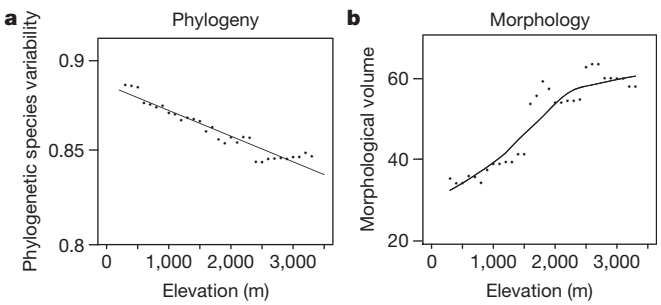

Figure 3 | Phylogenetic and morphological diversity along the elevational gradient. **a**, Estimate of phylogenetic relatedness[30] for all songbirds in a given elevational band; the line is the least-squares regression. On the scale, a value of 1 would imply a star phylogeny (that is, all species have independent history), whereas a value close to 0 implies that many species are closely related to each other. **b**, Volume of the convex hull for three morphological dimensions (see Extended Data Fig. 5a), as occupied by all songbirds in a given elevational band (the line is a nonparametric line fit; the outlier *Xiphirhynchus superciliaris* is omitted from this plot; its inclusion greatly steepens the slope).

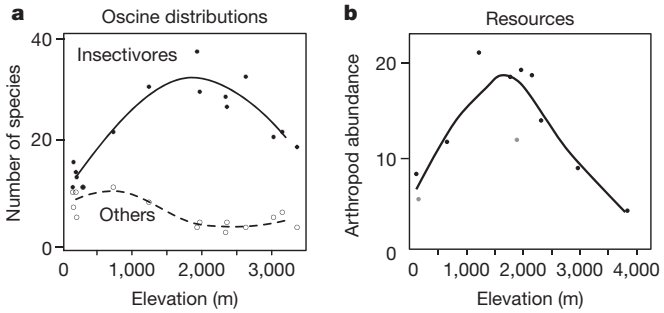

Figure 4 | Species richness and resource abundance. **a**, Number of breeding species censused on fifteen 5-hectare plots. **b**, Arthropod densities (from ref. 15, plus additional data (grey points)). Lines are nonparametric curve fits.

vegetation parameters and, for a subset of grids, we also measured arthropod densities. The mid-elevation peak in these 5-hectare plots (Fig. 4a) is very similar to that found at the larger scale (Fig. 1c). We found that this peak is entirely attributable to insectivorous species (Fig. 4a) and strikingly matches arthropod abundance (Fig. 4b). Arthropod abundance correlates with the total number of insectivorous individual birds on the 5-hectare grid (from 44 to 218; Pearson's correlation $r = 0.76$, the correlation with insectivorous bird biomass is $r = 0.75$) and the more insectivorous birds on the 5-hectare grid, the more insectivorous species were present ($r = 0.93$). A mid-elevation peak in arthropod abundance is surprising, given that both rainfall and temperature monotonically decline with elevation (Extended Data Fig. 8). However, mid-elevations are the lowest elevations that regularly freeze in winter and are therefore likely to experience a large leaf and arthropod flush in the spring. In addition, the lowest elevations contain many other insectivorous animals, potentially in competition with the songbirds. These include nonpasserine and suboscine birds (Fig. 1), an insectivorous ant (*Oecophylla smaragdina*, which is abundant at low elevations but absent at mid-elevations, personal observation of D.M.H. in 2011) and probably other poikilotherms.

In this continental environment, where species have had time to accumulate and dispersal barriers are relatively weak, both the appearance of new species and morphological diversification have substantially slowed and species distributions are well explained by abundance of resources. Rabosky and Matute[25] have demonstrated that, across clades, rates of evolution of reproductive isolation are generally decoupled from diversification rates. Our results imply that the ultimate limit on diversification is best explained, not by a slow rate of accumulation of reproductive isolation, but by the failure of species to expand ranges into new localities, which we attribute to competitive interactions. Because range expansions are essential to most ongoing speciation events[3], local interactions ultimately determine regional speciation rates, rather than regional speciation rates setting local diversity, as in many non-equilibrium models[26]. These results contrast with those from young environments, such as young archipelagoes[11]—which provide some of the best evidence for ongoing adaptive radiations—and with those from dispersal-limited, extinction-prone environments, notably islands—which provide some of the best evidence for bird communities below saturation[27].

METHODS SUMMARY

Tree construction. We obtained mitochondrial sequence data for all but one passerine species and nuclear data for 89%. We estimated a tree for the passerines and separately for 133 nonpasserines (all but 15 Himalayan species) from the following orders—the Piciformes, Bucerotiformes, Upupiformes, Trogoniformes, Coraciiformes, Cuculiformes, Psittaciformes, Apodiformes, Strigiformes and Columbiformes. For the primary analyses we constructed an ultrametric tree in BEAST[28], dated using multiple fossils and biogeographic dates, all set with uniform priors.

Morphology. We measured two or more specimens of each species in museums, drawing on males from within the study area whenever possible. We measured beak depth, beak length, beak width, tarsus length, and wing length. Mass and elevational distributions were based on the primary literature and our own fieldwork. In the main analyses we used ln(mass) and the first two principal components extracted

from the correlation matrix of residuals of regressions of ln(morphological traits) on ln(mass), all standardized to have unit variance (alternative approaches give similar results; see Extended Data Fig. 5).

Fieldwork. T.D.P. and D.M., plus up to two other experienced workers, independently censused birds in eighteen 5-hectare grids spanning the elevational gradient. In each grid two mornings were spent territory-mapping males, largely following the British Trust for Ornithology's common bird census protocols (http://www.bto.org) and assuming that the number of birds was twice the number of censused males.

Online Content Any additional Methods, Extended Data display items and Source Data are available in the online version of the paper; references unique to these sections appear only in the online paper.

Received 3 December 2013; accepted 24 March 2014.
Published online 30 April 2014.

1. Mayr, E. & Diamond, J. M. *The Birds of Northern Melanesia: Speciation, Ecology, and Biogeography* (Oxford Univ. Press, 2001).
2. Price, T. *Speciation in Birds* (Roberts, 2008).
3. Weir, J. T. & Price, T. D. Limits to speciation inferred from times to secondary sympatry and ages of hybridizing species along a latitudinal gradient. *Am. Nat.* **177,** 462–469 (2011).
4. Goldberg, E. E. & Lande, R. Ecological and reproductive character displacement on an environmental gradient. *Evolution* **60,** 1344–1357 (2006).
5. Harvey, P. H. & Rambaut, A. Comparative analyses for adaptive radiations. *Phil. Trans. R. Soc. Lond. B* **355,** 1599–1605 (2000).
6. Price, T. D. & Bouvier, M. M. The evolution of F1 postzygotic incompatibilities in birds. *Evolution* **56,** 2083–2089 (2002).
7. Rosenzweig, M. L. *Species Diversity in Space and Time* (Cambridge Univ. Press, 1995).
8. Endler, J. A. *Geographic Variation, Speciation, and Clines* (Princeton Univ. Press, 1977).
9. Chesson, P. Mechanisms of maintenance of species diversity. *Annu. Rev. Ecol. Syst.* **31,** 343–366 (2000).
10. Schluter, D. *The Ecology of Adaptive Radiation* (Oxford Univ. Press, 2000).
11. Grant, P. R. & Grant, B. R. *How and Why Species Multiply* (Princeton Univ. Press, 2008).
12. Yoder, J. B. *et al.* Ecological opportunity and the origin of adaptive radiations. *J. Evol. Biol.* **23,** 1581–1596 (2010).
13. Johansson, U. S. *et al.* Build-up of the Himalayan avifauna through immigration: a biogeographical analysis of the *Phylloscopus* and *Seicercus* warblers. *Evolution* **61,** 324–333 (2007).
14. Richman, A. D. & Price, T. Evolution of ecological differences in the Old World leaf warblers. *Nature* **355,** 817–821 (1992).
15. Ghosh-Harihar, M. & Price, T. D. A test for community saturation along the Himalayan bird diversity gradient, based on within-species geographical variation. *J. Anim. Ecol.* 628–638 (2014).
16. Jønsson, K. A., Fabre, P. H., Ricklefs, R. E. & Fjeldså, J. A major global radiation of corvoid birds originated in the proto-Papuan archipelago. *Proc. Natl Acad. Sci. USA* **108,** 2328–2333 (2011).
17. Päckert, M. *et al.* Horizontal and elevational phylogeographic patterns of Himalayan and Southeast Asian forest passerines (Aves: Passeriformes). *J. Biogeogr.* **39,** 556–573 (2012).
18. Kennedy, J. D. *et al.* Ecological limits on diversification of the Himalayan core Corvoidea. *Evolution* **66,** 2599–2613 (2012).
19. Price, T. D. The roles of time and ecology in the continental radiation of the Old World leaf warblers *(Phylloscopus* and *Seicercus). Phil. Trans. R. Soc. Lond. B* **365,** 1749–1762 (2010).
20. Wiens, J. J., Parra-Olea, G., Garcia-Paris, M. & Wake, D. B. Phylogenetic history underlies elevational biodiversity patterns in tropical salamanders. *Proc. R. Soc. Lond. B* **274,** 919–928 (2007).
21. Price, T. D. *et al.* Determinants of northerly range limits along the Himalayan bird diversity gradient. *Am. Nat.* **178,** S97–S108 (2011).
22. MacArthur, R. H. Patterns of species diversity. *Biol. Rev. Camb. Philos. Soc.* **40,** 510–533 (1965).
23. Ricklefs, R. E. Species richness and morphological diversity of passerine birds. *Proc. Natl Acad. Sci. USA* **109,** 14482–14487 (2012).
24. Rosenzweig, M. L. & Abramsky, Z. in *Species Diversity in Ecological Communities* (eds Ricklefs, R. E. & Schluter, D.) 52–65 (Univ. Chicago, 1993).
25. Rabosky, D. L. & Matute, D. R. Macroevolutionary speciation rates are decoupled from the evolution of intrinsic reproductive isolation in *Drosophila* and birds. *Proc. Natl Acad. Sci. USA* **110,** 15354–15359 (2013).
26. Cornell, H. V. Is regional species diversity bounded or unbounded? *Biol. Rev. Camb. Phil. Soc.* **88,** 140–165 (2013).
27. Ricklefs, R. E. & Bermingham, E. The concept of the taxon cycle in biogeography. *Glob. Ecol. Biogeogr.* **11,** 353–361 (2002).
28. Drummond, A. J. & Rambaut, A. BEAST: Bayesian evolutionary analysis by sampling trees. *BMC Evol. Biol.* **7,** 214 (2007).
29. Harmon, L. J., Weir, J. T., Brock, C. D., Glor, R. E. & Challenger, W. GEIGER: investigating evolutionary radiations. *Bioinformatics* **24,** 129–131 (2008).
30. Helmus, M. R., Bland, T. J., Williams, C. K. & Ives, A. R. Phylogenetic measures of biodiversity. *Am. Nat.* **169,** E68–E83 (2007).

Supplementary Information is available in the online version of the paper.

Acknowledgements We thank the government of India and the Chief Wildlife Wardens of the six Indian Himalayan states for permits. We also thank S. Dalvi, K. Jamdar, N. Jamdar, E. Scordato and D. Wheatcroft for help in the field, U. Borthakur and V. Mathur in the laboratory and E. Goldberg, R. Hudson, J. Kennedy, M. McPeek, A. Phillimore, D. Schluter, T. Tyrberg and J. Weir for advice. Tissue and toe pads for this project were provided by J. Cracraft (American Museum of Natural History), N. Rice (Academy of Natural Sciences, Philadelphia), M. Adams (The Natural History Museum, Tring), J. Dumbacher and M. Flannery (California Academy of Sciences), J. Bates and D. Willard (Field Museum of Natural History, Chicago), Herman Mays (Cincinnatti Museum); M. Wink (Institut für Pharmazie und Molekulare Biotechnologie, Heidelberg); R. Brumfeld and D. Dittmann (Lousiana State Museum of Zoology); S. Edwards (Museum of Natural History, Harvard); G. Frisk (Swedish Museum of Natural History, Stockholm); J. Dean and J. Rappole (National Museum of Natural History Smithsonian); S. Birks (Burke Museum, University of Washington); the Zoologisches Forschungmuseum Alexander Koenig, Bonn; J. Bolding Kristensen and J. Fjeldså (Zoological Museum, Copenhagen); the Zoologische Staatssammlung München, Munich; and K. Zyskowski (Yale University). This work was supported in part by grants from the US NSF and the National Geographic Society (TDP), the Jornvall Foundation, a Chinese Academy of Sciences Visiting Professorship (to P.A.), the Swedish Research Council (grants to U.O. and P.A.), the Wenner-Gren Foundation (a grant to U.S.J.), the Feldbausch Foundation of Mainz University (a grant to J.M.) and the German DFG (grants to B.H. and D.T.T., grant number Ti 679/1-1). We thank D. Tautz for making laboratory facilities available in Germany.

Author Contributions Study design and fieldwork: T.D.P. and D.M. Logistics: D.M. and P.S. Field collections: D.T.T., D.M.H., U.S.J., P.A., U.O., F.I., J.M., D.M. and T.D.P. Sequencing: D.M.H., U.S.J., D.T.T., U.O., P.A. and B.H. Arthropod censuses: M.G.-H. and T.D.P. Phylogeny construction: D.M.H., with early input from D.T.T. and P.A. Museum measurements: C.D.B., D.M., T.D.P. and U.S.J. Analysis and manuscript preparation: T.D.P., with input from B.H., D.M., D.M.H., D.T.T., P.A., U.S.J. and U.O.

Author Information Reprints and permissions information is available at www.nature.com/reprints. The authors declare no competing financial interests. Readers are welcome to comment on the online version of the paper. Correspondence and requests for materials should be addressed to T.D.P. (pricet@uchicago.edu).

METHODS

Conceptual basis and null models. This paper builds an estimate of the phylogenetic relationships of all members of a clade that are found in a locality, rather than the clade in total. Previous studies of adaptive radiations, defined here as divergence from a single ancestor to fill a variety of ecological niches[34], have studied clades, not communities, but these do not directly allow an assessment of how ecological differentiation—the essence of adaptive radiation—controls diversification and speciation.

The conceptual framework is illustrated in Extended Data Fig. 1, and follows refs 2, 3 and 35. Although adaptive radiation in young environments has been well studied, and connections between ecological diversification and reproductive isolation well established[36], little work has been done in older environments, which are a priori more likely to be ecologically full. As shown in Extended Data Fig. 1, the predictions are that speciation slows when ecological niches are filled, and the reason for this is that range expansions into sympatry become increasingly difficult. Range expansions may also slow because reproductive isolation is acquired more slowly when ecological opportunity is reduced (that is, different populations are now not under selection to adapt to different environments because niche space is increasingly filled up). However, even if populations are not subject to any divergent selection pressures at all, they should eventually differentiate to the level of full species. At that point, range expansions may remain difficult because of competition from the sister species (step 4 in Extended Data Fig. 1), as well as from other species in an environment where niches are increasingly occupied.

Our conclusions are that east Himalayan birds have approached this last step. If sympatric species were about the same age as the attainment of reproductive isolation, incomplete reproductive isolation may be limiting species accumulation. However, the average time to the common ancestor of pairs of close relatives (sisters on the assemblage tree) living in the sympatric assemblage is long (7 Myr). By contrast, postmating reproductive isolation in nature may typically be completed by 3 Myr since separation from their common ancestor (although complete loss of fertility in hybrids can evidently take longer than this[6]) because, first, many deleterious effects in hybrids are apparent by that time, which will lower fitness in the wild, and, second, hybrids between species often fall between niches occupied by the parental forms[2,10,11,36]. This reasoning applies to postmating isolation and it is possible that premating isolation remains incomplete. If so, complete loss of hybrid fitness plus ongoing hybridization would be a powerful means of setting range limits[4]. However, hybrid zones between species separated by more than 3 Myr are rare[2,3]. More specifically, in our extensive population studies of thousands of breeding pairs of songbirds in the western Himalayas[37], we have never observed hybridization events between species separated by more than 4 Myr. Further, we noted in the main text that 90% of the species absent from the study area do overlap with their closest relative in the study area somewhere in the Himalayas, implying that premating reproductive isolation is essentially complete between them.

We bolster the argument of limits through niche-filling by building a time-dated phylogeny of all species in the community, and find both a substantial slowdown in per-lineage rates of splitting within the phylogeny and a slowdown in morphological evolution over time. Both of these results are consistent with niche availability limiting diversification, but they need to be evaluated against a suitable null model:

Lineage splitting. A slowdown in lineage splitting refers to a less than exponential increase in species, as expected from a pure birth (Yule) model (a model with constant speciation and extinction leads to a greater-than-exponential increase[38]). A slowdown in lineage splitting has been observed in many studies of large clades[39] and has sometimes been interpreted as a consequence of niche-filling[40], as we do here. One bias is that there is a lag time to the production of allopatric forms that will then go on to be species, with the result that some of the recent splits in the phylogeny are not included when they should be[39,41,42]. Previous work has addressed this difficulty by simply lopping off the most recent branch length (for example, refs 39 and 41). An advantage of working with sympatric assemblages is that species are defined unambiguously, so the lag time to species recognition is not an issue. However, given allopatric/parapatric speciation, there must be a delay to sympatry that includes the following features: (1) development of reproductive isolation between allopatric forms, (2) dispersal across any barriers, and (3) establishment in the community. As can be seen from the plot of lineage diversification versus time in Fig. 2, and as quantified in Extended Data Table 1, a strong slowdown remains even if the phylogeny is truncated 3 Myr ago, which is surely longer than an appropriate null model for how long a lag time should be (it is longer than it has taken to produce the entire Darwin's finch radiation[2], which contains up to 11 sympatric species).

Sampling. One set of null models considers that the Himalayan assemblage represents a random sample from some larger region in which the Himalayas are embedded. A random sample of species from the tips results in a greater slowdown than is observed in the larger phylogeny, because deep nodes are generally captured, but shallow nodes often will not be[43]. Whether this is an appropriate null model is debatable (see below) but we test it in this section. We consider sampling from both all Asian oscines and the pure birth model, and find the downturn in the study area to be much stronger than expected on the basis of random sampling from these larger species pools, even if the plot of lineage versus time is truncated at 3 Myr ago (Extended Data Table 1). In addition, trees sampled from a larger species pool (based on the tree of Jetz *et al.*[31]) have ages of sisters not greatly different from those in the larger pool (4.5 Myr compared to about 4 Myr in the analyses of Extended Data Table 1), which is substantially shorter than is observed in the sympatric assemblage (see the 'Phylogeny construction' section, in which the tree of ref. 31 is compared to the oscine tree illustrated in Fig. 1b).

Given that neither a 3-Myr lag time to sympatry nor sampling can account for the strong slowdowns, we argue that the rejection of a constant diversification rate in the phylogeny of sympatric species results because more recently produced allopatric species find it increasingly difficult to invade the community, plus possibly there has also been a slowdown in the global production of species, which, by induction, is itself ultimately driven by the failure of range expansions. Because over 1,500 songbird species are present in Asia but only 358 are present in the study area, a failure of establishment (range expansions) clearly accounts for some of the long lag times.

Alternative null models. Despite the analyses reported in Extended Data Table 1, we suggest that random sampling from a larger phylogeny is not an appropriate null model if the goal is to assess ecological controls on species diversification. This is because most related allopatric forms reflect either ecological replacements, or responses to ecological diversity in other locations of the world and therefore are not part of an assemblage responding to local ecological controls. We illustrate the reasoning by considering one species present in the Himalayas, *Zosterops palpebrosus*, together with its closest sequenced relatives, as taken from the tree of ref. 31 (Extended Data Fig. 2).

Most of the members of the *Z. palpebrosus* clade (the clade containing the upper ten species in Extended Data Fig. 2) consist of allopatric forms, some of whom are quite young and may not be reproductively isolated, and all of which occupy an arboreal fruit-, flower- and insect-eating niche, and commonly forage in flocks, that is, are ecological equivalents in different locations. We suggest that young allospecies reflect species turnover within the same ecological niche[44], with extinction attributable to both small population size and recent climatic change, followed by colonization and population fragmentation creating peripheral forms. These allopatric forms would not be recognized as different species in the fossil record[45] and depend on expansion out of more stable refuges, such as the eastern Himalayas is inferred to have been[15,21]. This then suggests that a local-to-regional focus (stage 5 of Extended Data Fig. 1) as a limit on regional species numbers is at least as appropriate as the common regional-to-local focus as a limit on local diversity (compare ref. 46). The regional-to-local focus forms the basis for considering the local fauna to be a sample from the greater region, as tested in a previous section. However, if local interactions prevent the build-up of species in sympatry, the regional fauna is ultimately limited by local interactions, rather than the other way round.

Extended Data Fig. 2 also indicates some sympatry among *Zosterops* species. First, a pair of species on Reunion and Mauritius is thought to be the result of a double invasion[47] where one species *(Z. olivacea)* has become a flower specialist and is solitary[48]. Second, a clade of allopatric forms (the lower five species in Extended Data Fig. 2) contains some species sympatric with *Zosterops palpebrosus*. In sympatry, these species differ ecologically from *Z. palpebrosus*: in China, *Z. japonicus* is migratory, and species in the Indonesian islands are altitudinally segregated from *Z. palpebrosus*. Thus, these examples of sympatry may be considered a response to ecological conditions in different regions. Assessment of ecological controls on diversification would need to include both the timing of colonization and ecological amplitude in these regions.

Models of ecological controls. In young environments, a large diversity of niches may appear more or less simultaneously, with subsequent rapid diversification to fill these niches, as in classic examples such as cichlid fish and Darwin's finches. In other examples, opportunity may arise in pulses, or uniformly (for example, as a result of extinctions). Price[32] and Harvey and Rambaut[5] considered a simple model in which new niches arose uniformly through time (for example, as a result of an occasional extinction) and species evolve to occupy the new niche from the ecologically closest ancestor. As shown in Extended Data Fig. 3, this model creates a strong downturn in the lineage splitting pattern, as well as a burst of ecological and morphological diversification early in the radiation[32].

The results of the ecological controls model illustrated in Extended Data Fig. 3 are broadly consistent with the pattern we observe for lineage splitting and morphological evolution in the east Himalayan assemblage (Fig. 2). However, elevation does not show this pattern, with disparity accumulating relatively late. We suggest that the best interpretation is that a burst of ecological opportunity was relatively recently created along the elevation axis, in association with climate change 10 Myr

to 6 Myr ago[19] (the mammalian fossil record of Pakistan shows a high turnover across this period[49].)

Although morphological disparity in the 358 east Himalayan species phylogeny rapidly accumulates (Fig. 2, Extended Data Fig. 4), it still does so more slowly than the disparity curve of the simple niche-filling model illustrated in Extended Data Fig. 3. One contributing reason appears to be that the relatively recent appearance of high-elevation habitat creates opportunities along the other (body size and shape) axes, which are not always taken up by colonization from the ecologically most similar relative (an assumption of the model). A striking example is the high-elevation ground tit (*Pseudopodoces humilis*), which is the rightmost point in the tit clade of Fig. 2 (*Parus* and *Pseudopodoces,* shown in green). Far larger than other tits, *Pseudopodoces humilis* is morphologically convergent on low-elevation mynas: both *P. humilis* and mynas are predominantly open-country ground foragers. We speculate that climatic, habitat (absence of open areas at mid-elevations), and geographic barriers caused the 'open' niche at higher elevations to be not easily invaded by mynas, triggering the evolution of the ground tit from a tree-living *Parus.* This species is separated by an estimated 8 Myr from its closest relative in the study area, and the speciation occurred about the time high-elevation radiations were taking place in other groups 10–6 Myr ago (see Extended Data Fig. 6).

Significance tests of morphological evolution. For the main analysis in the text, we used the natural logarithm of mass—ln(mass)—and the first two principal components (PC1, PC2) from the residuals of ln(each morphological trait) on ln(mass), using the entire Himalayan oscine data set for which we have measurements, $N = 441$ species. Correlations with the original variables are in Extended Data Fig. 5. We standardized each of these three variables—ln(mass), PC1 and PC2—to have unit variance. The motivation for the standardization is that subtle differences in shape can have as much ecological significance as more obvious changes in size[14,18] making it more meaningful to give each equal weighting in morphological dispersion assessments. However, similar results on morphological volumes accrue if the values are unstandardized, in which case size becomes dominant.

The time course of morphological evolution is illustrated in Extended Data Fig. 4, replicating Fig. 2, but with diversification expected under the Brownian-motion model added. We used two methods to assess the significance of the slowdown in morphological evolution. First, we fitted two-rate Brownian-motion models for morphological traits to the east Himalayan oscine phylogeny using Geiger (Extended Data Fig. 5a, b). The two-rate model includes two additional parameters over the one-rate model: the breakpoint and the rate difference before and after the breakpoint. To account for uncertainty in tree topology in assessment of significance, we averaged likelihood scores over 100 trees sampled from the Bayesian posterior distribution of trees, and to assess significance we used the likelihood profile (Extended Data Fig. 5b).

In a second approach, we compared Ornstein–Uhlenbeck models to Brownian motion models (Extended Data Fig. 5c). This analysis was modified in several ways from the analysis in the previous paragraph. First, unlike the disparity plots (Fig. 2 and Extended Data Fig. 4) and the assessment in Extended Data Fig. 5a, we extracted three phylogenetically corrected principal-component scores[50] from the correlation matrix of the log-transformed morphological measurements, for the eastern oscine species alone ($N = 355$ species for which we have measurements, out of 358 species in total). The correlations ("revellePCs") with the original variables are in Extended Data Fig. 5d. We then asked at what point in time morphological evolution becomes constrained, by fitting Ornstein–Uhlenbeck and Brownian motion models to all clades subtended above a certain timeline, plus the one additional clade from the root to that timeline. In the Ornstein–Uhlenbeck models, all lineages subtending more than one species at each timeline were modelled with separate optima, but the constraining parameter was assumed to be the same for each clade (compare ref. 51). In all models the dispersive parameter was set the same throughout the tree. Relative weights of the two models were computed from the corrected (second-order) Akaike Information Criterion (AICc) scores obtained in the R program OUCH[52]. For both the Ornstein–Uhlenbeck and Brownian-motion models, at every timeline those lineages subtending just a single present-day species were removed before the analysis.

Both the tests indicate a strong slowdown in morphological evolution towards the present. This slowdown is not simply a result of a slowdown in lineage splitting, with morphological evolution concentrated at speciation events[53]. Over half of all speciation events occur after the slowdown in morphology has largely happened. These speciation events are often associated with elevation splits, ecological differences that are accompanied by relatively little morphological differentiation. As noted above, the slowdowns in morphological evolution are consistent with early diversification to fill niches associated with the major modes of life, as expected if ecological controls form the ultimate limit on species diversity and speciation.

Comparing morphology and elevation. The mid-point of elevation has evolved more recently than body size and body shape (Fig. 2, Extended Data Fig. 4). This is shown also by phylogenetic signal in the data, as measured using Blomberg's *K* value[54,55]. *K* is greater than 1 for size and shape (1.74 for size and 1.74 for shape, that is, close relatives are more similar than expected under the model of Brownian motion), and less than 1 for elevation (0.63, that is, there is more evolution in the terminal branches than expected under Brownian motion). Phylogenetic signal, as assessed by comparing the variance of phylogenetic contrasts in a randomization test[55] is significant for size and shape ($P = 0.02$), but not for elevation ($P = 0.07$).

To compare patterns of evolution for any pair of traits (for example, body size with elevation) we adapted the method of ref. 56. We computed the absolute values of the phylogenetic contrasts throughout the tree, and regressed them on node height: a positive value indicates more evolution at the tips. Regression slopes are negative for size and shape and positive for elevation. We then compared the slopes of the regressions with two-sample Student's *t*-tests (with 351 degrees of freedom, as morphology was not available for four of the 358 species, implying 353 contrasts). The results were: size versus elevation, $t = 3.9$, two-tailed $P < 0.001$; size versus shape, $t = 1.34$, $P = 0.18$; and shape versus elevation, $t = 2.8$, $P = 0.006$. All traits were standardized to unit variance before the analysis, to remove scale effects.

Phylogeny construction. For taxonomic sampling, we incorporated all 461 oscines, all 5 suboscines and 133 of the 149 nonpasserines (from the Piciformes, Bucerotiformes, Upupiformes, Trogoniformes, Coraciiformes, Cuculiformes, Psittaciformes, Apodiformes, Strigiformes and Columbiformes, excluding Galliformes, Anseriformes and Falconiformes) found in the Himalayas[21,57]. The resulting data set includes over 120 species sequenced for the first time, including rare species such as the Bugun liocichla *(Liocichla bugunorum),* known only from a few pairs. We also included 37 non-Himalayan species for the purpose of time-calibration (see source data for Fig. 1). Taxonomy follows ref. 57, except as outlined in the source data file associated with Fig. 1.

The majority of new sequences in this study were amplified using tissues sourced from museum collections or from feathers and blood collected in the field. However, we had to rely exclusively upon material from toe-pads for 54 species (31 passerines and 23 nonpasserines) without available fresh material. Owing to the degraded nature of DNA in these samples, amplification of mitochondrial loci proved difficult and nuclear data often impossible (see DNA extraction, amplification and sequencing). To alleviate this limitation and maximize the amount of data used for phylogenetic analyses, in some cases we incorporated genetic data from non-Himalayan surrogate species. We incorporated sequence data from surrogate species, as listed in the source data for Fig. 1, according to three different rationales: (1) if a species was the only member of its genus in the Himalayas we used an extra-limital congener; (2) if a species' genus contained more than one species in the Himalayas but the non-Himalayan sister species of that particular species was clear and (3) if a genus was not monotypic in the Himalayas and no locus-specific data for that genus was available for any of its Himalayan members, locus data from a non-Himalayan representative was assigned to a single Himalayan representative.

For example, the genus *Oriolus* contains four species that inhabit the Himalayas, for none of which we had adequate material to amplify the *RAG1* locus and none of which have sequence data for the *RAG1* locus on GenBank. Here, we added *RAG1* from the non-Himalayan *Oriolus cruentus* for the Himalayan *Oriolus kundoo* because we have no other RAG1 data for this genus (rationale 3). Rationale 3 makes the assumption that the genus in question is monophyletic, which is most likely to be the case when further qualified by rationale 2. To assess whether the use of genetic data from surrogate species induced a bias in phylogenetic reconstruction, we repeated the phylogenetic analyses outlined below with all surrogate information removed. No bias was detected.

DNA extraction, amplification, and sequencing. DNA was extracted using Qiagen DNEasy Blood and Tissue kits (Qiagen) according to the manufacturer's instructions. Museum tissue and toe-pad materials were digested overnight in a mixture of 180 µl ATL buffer and 20 µl proteinase-K and then eluted with 200 µl or 50 µl of AE buffer respectively, following the manufacturer's instructions. We sequenced the mitochondrial cytochrome b gene (*cytb*), the mitochondrial NADH dehydrogenase subunit 2 (*ND2*), intron 2 of the myoglobin gene, introns 6 and 7 of the ornithine decarboxylase (*ODC*) gene, intron 11 of the glyceraldehyde-3-phosphodehydrogenase (*GAPDH*) gene, and the recombination activating protein 1 (*RAG1*) gene—partial coding sequences. The six loci were amplified and sequenced using standard primers and amplification profiles as described in ref. 58 for mitochondrial cytochrome *b*, by M. D. Sorenson *et al.* (http://people.bu.edu/msoren/primers.html) for mitochondrial *ND2,* ref. 59 for *myoglobin* and *GAPDH,* and ref. 60 for *RAG1.* We designed new primers to amplify the *ODC* locus for this study. Toe-pad samples were amplified as needed with a series of short, overlapping fragments of 200–600 base pairs, using a large set of genera-specific internal primers. All primers used in this study are available for use on request. Polymerase chain reaction (PCR) products were cleansed using ExoSap IT and sequenced directly on an ABI3730XL capillary sequencer.

Phylogenetic analyses. Sequences for each locus were aligned using MAFFT v7.1 (http://mafft.cbrc.jp/alignment/software/). Some manual adjustment was necessary

for nuclear sequences. Indels that were specific to a single species within the alignment were removed to reduce noise. The best-fitting model for each locus was identified with the AIC implemented in MrModelTest2 v2.3 (ref. 61), in conjunction with PAUP* (ref. 62), as follows: GTR+G for *cytb* and *myoglobin*; GTR+I+G for *ND2, ODC,* and *RAG1*; and HKY+G for *GAPDH*.

A time-calibrated phylogeny of the Himalayan Passeriformes was estimated by Bayesian inference using BEAST v1.8 (ref. 28) with computational assistance from BEAGLE v2.0 (ref. 63). For computational reasons, we ran the passerines (including the suboscines) largely independently from the remaining nonpasserines. Some species were included in both runs to help with time-calibration. Each locus was assigned its own partition with unlinked substitution and clock models but with a linked tree model. Thirteen time calibrations were used to date the tree. All dates were modelled with a uniform prior. Biogeographic calibrations were modelled between the date of geographic activity and the present to place a maximum age boundary. Fossil calibrations were modelled between 80.0 million years ago and the date of the fossil to place a minimum age boundary. By using multiple calibration points scattered broadly throughout the tree, we expect the accuracy of age calibration to improve as the average distance between calibrated and uncalibrated nodes decreases[64]. We ran BEAST for 50 million generations sampling every 5,000 generations for a total of 10,000 trees. We assessed run performance and determined appropriate burn-in length using Tracer v1.5 (ref. 65) and constructed the maximum-likelihood clade credibility tree using TreeAnnotator v1.8 (ref. 28). Ten of the 13 time calibrations in the passerine part of the tree have been independently verified to be appropriate for use[66]. We confirmed the additional three age calibrations using methods similar to those of ref. 66.

For the main phylogeny illustrated in Fig. 1b, a time-calibrated nonpasserine tree was run using the same BEAST methods, as described above. We constrained the order-level topology according to ref. 67 both because of the difficulty of achieving accurate order-level resolution with our limited data set and also because these deeper relationships are beyond the scope of this paper. We incorporated 11 time calibrations, three of which were also used for the oscine tree, using the same uniform prior logic for fossil and biogeographic calibrations. We spliced together the Passeriformes and nonpasserine trees using APE[68], based on the several passerine species included in the nonpasserine tree. Additional phylogeny appendices are available as follows: (1) passerine and nonpasserine trees submitted to http://treebase.org (http://purl.org/phylo/treebase/phylows/study/TB2:S15660); (2) the XML file used to create the passerine tree in BEAST (Supplementary Information).

The Jetz *et al.*[31] tree. The global tree of birds by ref. 31 includes all the species we studied here. However, among the 358 oscines in the eastern square, 85 species in their tree were without sequence data and were inserted into an assigned clade based on taxonomy, using the pure birth (Yule) model and nearly all the other species had less sequence data than we used. In our investigations we computed a maximum clade credibility tree on a sample of 100 trees ('Hackett backbone') downloaded from http://birdtree.org. The portion of the tree[31] that includes the species we studied differs in several respects from ours and shows a much smaller slowdown in lineage-splitting events towards the present (the splitting-rate correlation coefficient $r = 0.13$ lineages per lineage per Myr over the first third of the tree to $r = 0.09$ to $r = 0.085$ over the last third; this compares with $r = 0.27$, $r = 0.13$ and $r = 0.06$ in the presented tree). The difference appears to be for at least three reasons: (1) the much older root of the oscines in the tree of ref. 31 (53 Myr ago versus 34 Myr ago in the current one), (2) the tree of ref. 31 inserted 25% of the species using the pure birth model because no sequence data at all was available and (3) taxonomy is a poor guide to where these species should be inserted.

The much older root in the tree of ref. 31 probably stems from the use of old fossils (in their analysis, young calibration dates could not be used, given the way clades were inserted into a backbone tree) and perhaps the use of log-normal priors, which gives undue weight to point estimates. The age for the root is incongruent with the fossil record, plus there is a relative lack of passerine morphological diversity[69]. The root of the Eurasian species in our tree dates precisely to the Oligocene/Eocene boundary (34 Myr ago), a period of extreme cooling with a drop of several degrees Celsius in the oceans over a short time[70], and large turnover in the Asian mammalian fossil record[71]. It is therefore in accord with the idea that ecological opportunity drove songbird diversification.

Despite the conflicts between trees, a critical result on the age of 'sisters' (closest relatives on the phylogeny of the 358 sympatric oscine species) is consistent: the average age of sister pairs in the tree from ref. 31 (7 Myr $\pm$ 0.47 Myr, $N = 112$ sisters, with 9 pairs separated by less than 2 Myr) is similar to that in the tree presented here (7.1 Myr $\pm$ 0.3 Myr, $N = 116$, with 3 pairs separated by less than 2 Myr). The great age of Himalayan species appears to be robust.

Estimating diversity along the elevational gradient. For Fig. 3a we used the phylogenetic species diversity measure of Helmus and Ives[30,72] because it captures phylogenetic structure in a way that is insensitive to phylogeny size. A value of 1 is equivalent to a star phylogeny, whereas a value close to zero indicates that many species are close relatives. We pruned the larger phylogeny to a smaller one that connects all species thought to be in a particular elevational belt, based on overlapping altitudinal ranges (see source data for Fig. 2). Results were similar if we used species present in our censuses of 5-hectare plots instead.

In Extended Data Fig. 6 we show the plot of lineage versus time for the 500 m and 3,000 m elevation, both of which are estimated to contain the same number of species. The plot is cast on a linear scale to highlight the differences. The lower elevation has a more rapid accumulation of species from 20 Myr ago to 10 Myr ago, whereas the higher elevation has a more rapid accumulation from 10 Myr ago to 6 Myr ago. Note that although the higher elevation consists of younger species, very few species accumulate at either location over the past 6 Myr.

For Fig. 3b, as in the case of the phylogenetic diversity measure, we used all species thought to be in a particular elevational belt, based on overlapping altitudinal ranges. However, results were similar if we used species present in our censuses of 5-hectare plots instead (Extended Data Fig. 7). The volume of the convex hull was computed in morphological 3-space (Extended Data Fig. 5A, D) using the library FD[73,74]. The convex hull is sensitive to sample size, hence is conservative with respect to the main finding (higher volume at higher altitudes, even though species numbers are less than at middle altitudes). A measure insensitive to sample size (summed variance of the three dimensions) gave congruent results (not shown). In Extended Data Fig. 7 we show morphological space on the first two dimensions at four locations. At highest elevations, both the shape and size dimensions are greatest, which may partly reflect an absence of nonpasserine competitors[18] as well as more open habitat, which favours a relatively long tarsus.

Field methods. The 'study area' is bounded by the coordinates 88° E, 93.1° E, 26.3° N and 28.1° N, covers an area of 10,389 km^2, and spans an elevational range from 37 m to 6,778 m. Essential climatic features are illustrated in Extended Data Fig. 8. Temperature, precipitation and estimated productivity decline monotonically with elevation (Extended Data Fig. 8; ref. 75). Precipitation shows the greatest spatial variation at low elevations (Extended Data Fig. 8).

T.D.P. and D.M. collected data over an elevational range of 150–4,100 m in six field seasons (2007–2012, mostly in the later years), preceded by three (T.D.P.) or more (D.M.) earlier visits to familiarize ourselves with the birds. We worked entirely in India, with no visits to Bhutan, and set up 5-hectare grids using the Global Positioning System (GPS) in as undisturbed forest as possible, usually over 2 km from any substantial clearing. Locations of the grids are plotted in Extended Data Fig. 8, as listed in the Source Data for Fig. 4. Two observers walked slowly over a grid for two mornings during the breeding season, from dawn for about 4 h, mapping singing males and recording sightings. For the more common species, concordance among observers in the number of singing males was high. Although only one observer often recorded one or other of the uncommon species, both observers recorded similar numbers of species in total. We assume that a single observer's record approximates breeding birds on the grid (that is, rare species which were seen by one or other of us are often at lower density than 1 pair per 5 hectares and some are unlikely to be breeding on the grid.) We analysed the surveys of T.D.P. and the surveys of D.M. plus assistants separately and got similar results. T.D.P.'s surveys are reported (see source data for Fig. 4 for the listing of surveys included). M.G.-H. collected arthropod data on or near nine of the grids, during three separate visits[76,77]. Methods usually involved placing fifty 200-litre garbage bags over lower branches, breaking the branch, anesthetizing the arthropods and then sorting through the bag (see ref. 77 for standard errors.) Because not all grids were surveyed in this way, we used a quadratic curve fit to predict numbers of arthropods at a given elevation. The relatively few arthropods at low elevations were unexpected, so in May 2013, we made additional collections at a new site, plus some additional collections at site B1. See the source data for details on these collections. Vegetation data were collected on each grid[21] and are also reported in the source data for Fig. 4. The smoothed lines in Fig. 4 were fitted using the lowess procedure in R (http://stat.ethz.ch/R-manual/R-patched/library/stats/html/lowess.html).

Mid-elevation peak in species richness. Species richness at the 2-km^2 scale was estimated using the same raster as the http://worldclim.org 2.5-arcminutes resolution, which resulted in 5,246 squares across the study area. The points represent the total number of breeding species estimated for each square. To assign a species to a square, we derived its east and west range limits along the Himalayas from the maps of Rasmussen and Anderton[57] (as described in ref. 21), and its altitudinal limits from our own work (source data for Fig. 2). Smooth lines in Fig. 1 are General Additive Model (gam) fits using the mgcv library in R (http://cran.r-project.org/web/packages/mgcv/index.html). Critical additional packages used to construct that figure were Sp[78,79], Raster[80] and PBSmapping[81].

Rahbek[82] drew attention to the presence of a peak in bird species richness at mid-elevations, rather than a monotonic decline in species numbers with elevation. In a survey of 78 bird studies McCain[83] found that about half showed a mid-elevation peak. Several ecological explanations have been presented. Rahbek[82] noted that mid-elevations in the neotropics have increased structural diversity, notably epiphytes,

McCain[83] found that species numbers often correlate with productivity (mountains that are dry at the base are those that tend to have mid-elevation peaks), Rosenzweig and Abramsky[24] noted more generally that some mid-elevation peaks may arise even if productivity declines, owing to competition with other groups, and Terborgh[84] showed that different guilds have different elevational patterns, which he related to different resource distributions. Our interpretation of the Himalayan gradient is consistent with available resources being the ultimate driver of the peak. The mid-elevation peak is restricted to insectivorous oscines, which is related to arthropod abundance: this in turn may result from both climatic factors (for example, a spring flush of leaf) and the presence of efficient competitors at lower elevations. However, several other hypotheses for the mid-elevation peak have been proposed[85]. First, larger areas may accumulate more species[82]. Within the study area (Extended Data Fig. 8), the area within 500-m bands (between elevations of 200 m and 3,700 m) is roughly similar, albeit with a slight mid-elevation peak (Extended Data Fig. 9a), but overall the low elevations (Indian plains) and the high elevations (Tibetan plateau) have much more area than the middle elevations. Three other hypotheses, not described in the main text, are considered in more detail.

The first is a concern with data. If estimates of elevational ranges are simply based on connecting the highest and lowest records of a species (so-called range-through methods), then as one approaches the domain boundaries sampling error inevitably means that some species are missed[86]. Our 5-hectare plot surveys are unaffected by this issue and these local estimates match the integrated elevational distributions (compare Figs 1 and 4). Further, elevational ranges are unlikely to be underestimates of the true ranges because (1) they integrate over multiple years, publications and elevational gradients and (2) isolated breeding birds beyond their normal range limits may be especially recorded in the literature. Reason (2) means that it is conceivable that our ranges are over-estimated, but we have done our best to eliminate this on the basis of our field experiences.

The second concern is that of a suitable null model against which to assess the mid-elevation peak. In one much-discussed model, whose null character has been debated[87,88], shuffling ranges of fixed sizes on a bounded domain inevitably leads to more species at mid-elevations[89]. Some other null models give weak or no mid-elevation peaks[86]. In the original null model a prominent peak at mid-elevations is most expected if elevational ranges are a medium to large fraction of the total domain[83]. In our study, oscine elevational ranges average 1,154 m, which is about a quarter of the distance from the plains to the treeline (just 32 of the 96 oscines at 700 m are also found at 1,900 m and of the 155 at 1,900 m only 30 are also at 3,100 m; none of the species at 700 m are also at 3,100 m). The original mid-domain null model results in zero species at the boundaries[90]. We simulated this version, sampling species range mid-points on the domain size most favourable for the null hypothesis (200 m, 3,800 m) and obtaining mean R^2 associations of real and simulated data of 0.66, when richness was evaluated at every 100 m. Regions at the extremes lay above the 95% confidence limits from the simulated data and the whole transect between 1,000 m and 3,000 m lay below the null model confidence limits; a relatively poor fit. Because species distributions spread into south India and a long way above the treeline it is unclear what domain size to use: tests on larger domain sizes gave lower R^2 values. The mid-domain null has been generally rejected across bird studies[83], including an application to the bird diversity gradient in the eastern Himalayas[75] and is clearly not compatible with the distributions of nonpasserines and those songbirds that are not insectivores, both of which show monotonic declines from low elevations (Figs 1 and 4).

An important issue is whether the mid-elevation peak represents a "mass effect" whereby some species in a particular location are only present because of dispersal[91], that is, they represent sink populations, which could not be maintained in the absence of immigration. In theory, species can disperse from both above and below at intermediate elevations but only from one direction closer to the domain edges. This may lead to a mid-elevation peak, with local plots saturated to similar levels but those at mid-elevations having excess sink species, that is, sink species[92] occur to a greater extent in the mid-elevations. To address this, we focused on the local (grid) surveys, which show a mid-elevation peak comparable to that at the larger scales (Fig. 4a). We listed as plausible candidates for sink species all species represented by just a single breeding pair and which were under 300 m from either their upper or their lower elevational range limit (except in the case of grids below 300 m, when we used the criteria that these species should not extend south of the Himalayas into the plains or Assam hills). By this measure, up to 12 species at mid-elevations may be sink species. However, at elevations below 200 m up to 8 species may be sink species. If we remove sink species, the mid-elevation peak remains prominent (Extended Data Fig. 9b).

The mid-elevation peak is attributed mostly to a large number of small species (<15 g). This pattern is consistent with a large number of small arthropods at these elevations[77]. At lower elevations, arthropod distributions are skewed towards larger sizes, and insectivores are also generally larger. Our hypothesis, following ref. 24, is that a large abundance of arthropods permits finer subdivision of the niche. Terborgh and Faaborg[93] noted that insectivores may more generally be able to achieve fine niche partitioning, and this may well not be reflected in large morphological differences.

31. Jetz, W., Thomas, G. H., Joy, J. B., Hartmann, K. & Mooers, A. O. The global diversity of birds in space and time. *Nature* **491,** 444–448 (2012).
32. Price, T. Correlated evolution and independent contrasts. *Phil. Trans. R. Soc. Lond. B* **352,** 519–529 (1997).
33. Hijmans, R. J., Cameron, S. E., Parra, J. L., Jones, P. G. & Jarvis, A. Very high resolution interpolated climate surfaces for global land areas. *Int. J. Climatol.* **25,** 1965–1978 (2005).
34. Losos, J. B. Adaptive radiation, ecological opportunity, and evolutionary determinism. *Am. Nat.* **175,** 623–639 (2010).
35. Mayr, E. *Systematics and the Origin of Species from the Viewpoint of a Zoologist* (Columbia Univ. Press, 1942).
36. Nosil, P. *Ecological Speciation* (Oxford Univ. Press, 2012).
37. Price, T., Zee, J., Jamdar, K. & Jamdar, N. Bird species diversity along the Himalayas: a comparison of Himachal Pradesh with Kashmir. *J. Bombay Nat. Hist. Soc.* **100,** 394–409 (2003).
38. Harvey, P. H., May, R. M. & Nee, S. Phylogenies without fossils. *Evolution* **48,** 523–529 (1994).
39. Phillimore, A. B. & Price, T. D. Density-dependent cladogenesis in birds. *PLoS Biol.* **6,** 483–489 (2008).
40. Phillimore, A. B. & Price, T. D. in *Speciation and Patterns of Diversity* (eds Butlin, R. K., Bridle, J. & Schluter, D.) 240–256 (Cambridge Univ. Press, 2009).
41. Weir, J. T. Divergent patterns of species accumulation in lowland and highland neotropical birds. *Evolution* **60,** 842–855 (2006).
42. Etienne, R. S. & Rosindell, J. Prolonging the past counteracts the pull of the present: protracted speciation can explain observed slowdowns in diversification. *Syst. Biol.* **61,** 204–213 (2012).
43. Pybus, O. G. & Harvey, P. H. Testing macro-evolutionary models using incomplete molecular phylogenies. *Proc. R. Soc. Lond. B* **267,** 2267–2272 (2000).
44. McPeek, M. A. The ecological dynamics of clade diversification and community assembly. *Am. Nat.* **172,** E270–E284 (2008).
45. Rabosky, D. L. Diversity-dependence, ecological speciation, and the role of competition in macroevolution. *Annu. Rev. Ecol. Evol. Syst.* **44,** 481–502 (2013).
46. Ricklefs, R. E. Community diversity: relative roles of local and regional processes. *Science* **235,** 167–171 (1987).
47. Coyne, J. A. & Price, T. D. Little evidence for sympatric speciation in island birds. *Evolution* **54,** 2166–2171 (2000).
48. Gill, F. B. Ecology and evolution of sympatric Mascarene white-eyes, *Zosterops borbonica* and *Zosterops olivacea*. *Auk* **88,** 35–60 (1971).
49. Badgley, C. *et al.* Ecological changes in Miocene mammalian record show impact of prolonged climatic forcing. *Proc. Natl Acad. Sci. USA* **105,** 12145–12149 (2008).
50. Revell, L. J. Size-correction and principal components for interspecific comparative studies. *Evolution* **63,** 3258–3268 (2009).
51. Beaulieu, J. M., Jhwueng, D. C., Boettiger, C. & O'Meara, B. C. Modeling stabilizing selection: expanding the Ornstein-Uhlenbeck model of adaptive evolution. *Evolution* **66,** 2369–2383 (2012).
52. Butler, M. A. & King, A. A. Phylogenetic comparative analysis: a modeling approach for adaptive evolution. *Am. Nat.* **164,** 683–695 (2004).
53. Ricklefs, R. E. Cladogenesis and morphological diversification in passerine birds. *Nature* **430,** 338–341 (2004).
54. Blomberg, S. P., Garland, T. & Ives, A. R. Testing for phylogenetic signal in comparative data: behavioral traits are more labile. *Evolution* **57,** 717–745 (2003).
55. Kembel, S. W. *et al.* Picante: R tools for integrating phylogenies and ecology. *Bioinformatics* **26,** 1463–1464 (2010).
56. Mahler, D. L., Revell, L. J., Glor, R. E. & Losos, J. B. Ecological opportunity and the rate of morphological evolution in the diversification of Greater Antillean Anoles. *Evolution* **64,** 2731–2745 (2010).
57. Rasmussen, P. C. & Anderton, J. C. *Birds of South Asia: the Ripley Guide* (Lynx, 2005).
58. Weir, J. T. & Schluter, D. The latitudinal gradient in recent speciation and extinction rates of birds and mammals. *Science* **315,** 1574–1576 (2007).
59. Dong, F., Li, S. H. & Yang, X. J. Molecular systematics and diversification of the Asian scimitar babblers (Timaliidae, Aves) based on mitochondrial and nuclear DNA sequences. *Mol. Phylogenet. Evol.* **57,** 1268–1275 (2010).
60. Groth, J. G. & Barrowclough, G. F. Basal divergences in birds and the phylogenetic utility of the nuclear RAG-1 gene. *Mol. Phylogenet. Evol.* **12,** 115–123 (1999).
61. Nylander, J. A. A., Ronquist, F., Huelsenbeck, J. P. & Nieves-Aldrey, J. L. Bayesian phylogenetic analysis of combined data. *Syst. Biol.* **53,** 47–67 (2004).
62. Swofford, D. L. *PAUP*. Phylogenetic Analysis Using Parsimony (*and other methods)* Version 4 (Sinauer, 2003).
63. Ayres, D. L. *et al.* BEAGLE: an application programming interface and high-performance computing library for statistical phylogenetics. *Syst. Biol.* **61,** 170–173 (2012).
64. Linder, H. P., Hardy, C. R. & Rutschmann, F. Taxon sampling effects in molecular clock dating: an example from the African Restionaceae. *Mol. Phylogenet. Evol.* **35,** 569–582 (2005).
65. Rambaut, A. & Drummond, A. J. *Tracer* v1.4 http://beast.bio.ed.ac.uk/ (2007).
66. Weir, J. T. & Schluter, D. Calibrating the avian molecular clock. *Mol. Ecol.* **17,** 2321–2328 (2008).
67. Hackett, S. J. *et al.* A phylogenomic study of birds reveals their evolutionary history. *Science* **320,** 1763–1768 (2008).
68. Paradis, E., Claude, J. & Strimmer, K. APE: analyses of phylogenetics and evolution in R language. *Bioinformatics* **20,** 289–290 (2004).

69. Mayr, G. The age of the crown group of passerine birds and its evolutionary significance—molecular calibrations versus the fossil record. *Syst. Biodivers.* **11,** 7–13 (2013).
70. Hansen, J. *et al.* Target atmospheric CO_2: where should humanity aim? *Open Atmos. Sci. J.* **2,** 217–231 (2008).
71. Kraatz, B. P. & Geisler, J. H. Eocene-Oligocene transition in Central Asia and its effects on mammalian evolution. *Geology* **38,** 111–114 (2010).
72. Helmus, M. R. & Ives, A. R. Phylogenetic diversity-area curves. *Ecology* **93,** S31–S43 (2012).
73. Laliberté, E. & Legendre, P. A distance-based framework for measuring functional diversity from multiple traits. *Ecology* **91,** 299–305 (2010).
74. Laliberté, E. & Shipley, B. FD: measuring functional diversity from multiple traits, and other tools for functional ecology. *R package* version 1. 0-11, http://cran.r-project.org/web/packages/FD/index.html (2011).
75. Acharya, B. K., Sanders, N. J., Vijayan, L. & Chettri, B. Elevational gradients in bird diversity in the eastern Himalaya: an evaluation of distribution patterns and their underlying mechanisms. *PLoS ONE* **6,** e29097 (2011).
76. Gross, S. & Price, T. Determinants of the northern and southern range limits of a warbler. *J. Biogeogr.* **27,** 869–878 (2000).
77. Ghosh-Harihar, M. Distribution and abundance of foliage-arthropods across elevational gradients in the east and west Himalayas. *Ecol. Res.* **28,** 125–130 (2013).
78. Pebesma, E. J. & Bivand, R. S. Classes and methods for spatial data in R. *R News* **5,** http://cran.r-project.org/doc/Rnews/ (2005).
79. Bivand, R. S., Pebesma, E. J. & Gomez-Rubio, V. *Applied Spatial Data Analysis with R.* (Springer, 2008).
80. Hijmans, R. J. & van Etten, J. Raster: geographic analysis and modeling with raster data. *R package* version 1. 9-92, http://CRAN.R-project.org (2011).
81. Schnute, J. T., Boers, N. M. & Haigh, R. PBS Mapping 2: user's guide. *Can. Tech. Rep. Fish. Aquat. Sci.* **2549,** 126 (2004).
82. Rahbek, C. The elevational gradient of species richness—a uniform pattern. *Ecography* **18,** 200–205 (1995).
83. McCain, C. M. Global analysis of bird elevational diversity. *Glob. Ecol. Biogeogr.* **18,** 346–360 (2009).
84. Terborgh, J. Bird species diversity on an Andean elevational gradient. *Ecology* **58,** 1007–1019 (1977).
85. Sanders, N. J. & Rahbek, C. The patterns and causes of elevational diversity gradients. *Ecography* **35,** 1–3 (2012).
86. Grytnes, J. A. & Vetaas, O. R. Species richness and altitude: a comparison between null models and interpolated plant species richness along the Himalayan altitudinal gradient, Nepal. *Am. Nat.* **159,** 294–304 (2002).
87. Hawkins, B. A., Diniz, J. A. F. & Weis, A. E. The mid-domain effect and diversity gradients: is there anything to learn? *Am. Nat.* **166,** E140–E143 (2005).
88. Zapata, F. A., Gaston, K. J. & Chown, S. L. The mid-domain effect revisited. *Am. Nat.* **166,** E144–E148 (2005).
89. Colwell, R. K., Rahbek, C. & Gotelli, N. J. The mid-domain effect: there's a baby in the bathwater. *Am. Nat.* **166,** E149–E154 (2005).
90. McCain, C. M. The mid-domain effect applied to elevational gradients: species richness of small mammals in Costa Rica. *J. Biogeogr.* **31,** 19–31 (2004).
91. Grytnes, J. A., Heegaard, E. & Romdal, T. S. Can the mass effect explain the mid-altitudinal peak in vascular plant species richness? *Basic Appl. Ecol.* **9,** 373–382 (2008).
92. White, E. P. & Hurlbert, A. H. The combined influence of the local environment and regional enrichment on bird species richness. *Am. Nat.* **175,** E35–E43 (2010).
93. Terborgh, J. W. & Faaborg, J. Saturation of bird communities in the West Indies. *Am. Nat.* **116,** 178–195 (1980).

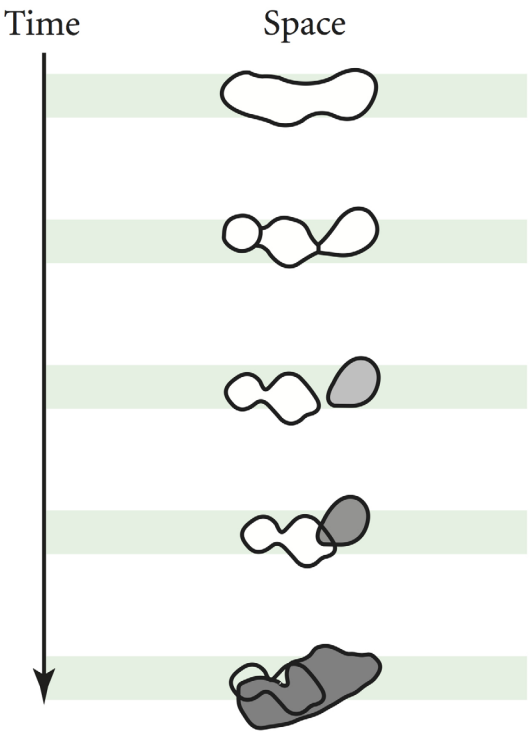

Extended Data Figure 1 | The speciation cycle. A species distributed across space becomes fragmented as a result of either vicariance (illustrated) or dispersal. After barrier formation, reproductive isolation develops. For the cycle to continue at least one of the species must expand into the other's range, which requires reproductive isolation, and generally also ecological compatibility.

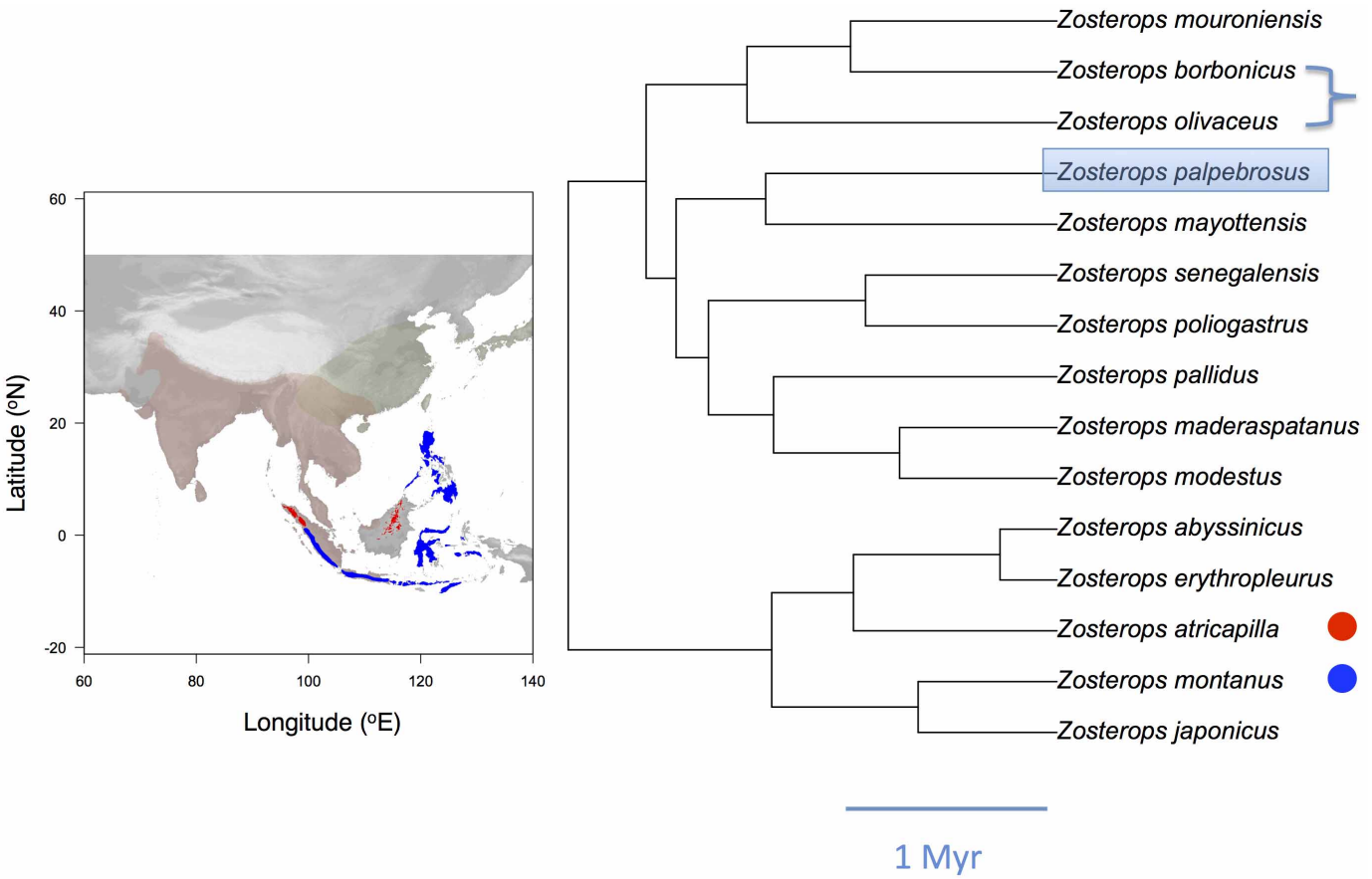

Extended Data Figure 2 | Close relatives of a single Himalayan species, the Oriental white-eye, *Zosterops palpebrosus.* Only species for which sequence data are available are included (tree from ref. 31). The range of *Z. palpebrosus* (light red) overlaps with members of the clade containing the lower 5 species, for example, with *Z. japonicus* (which is migratory) (light green) in eastern China and *Z. atricapilla* (red) and *Z. montanus* (blue) in Indonesia, where *Z. palpebrosus* is altitudinally segregated from them. Within the *Z. palpebrosus* clade, all species are allopatric replacements, except for the two species on the Mascarene Islands (bracketed). The timeline is from ref. 31.

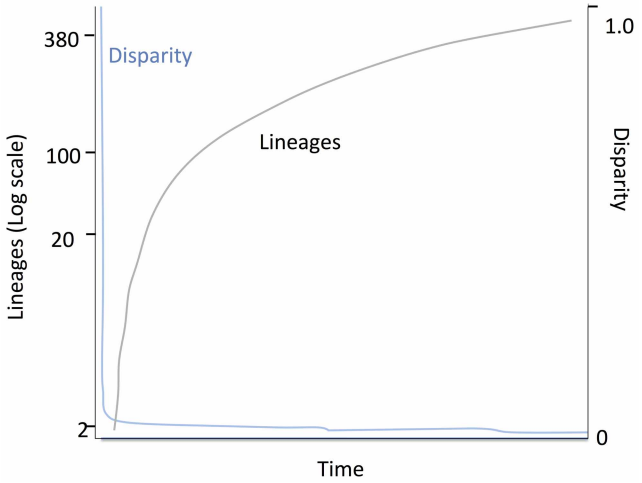

Extended Data Figure 3 | Plot of lineage versus time and morphological disparity generated in a simple model of ecological controls[32]. In this model, new niches appear uniformly through time, and new species arise to fill them, with the criterion that new species are always derived from the ecologically most similar form[5,32]. For this simulation, the position of a new niche was drawn from a bivariate normal (x, y) with a correlation of 0.5, with 380 niches appearing sequentially and uniformly spaced in time. The result is a linear accumulation of species through time (that is, a downturn on the log scale), and most of the morphological variation accumulating early in the radiation (in the plot, disparity for one variable is shown).

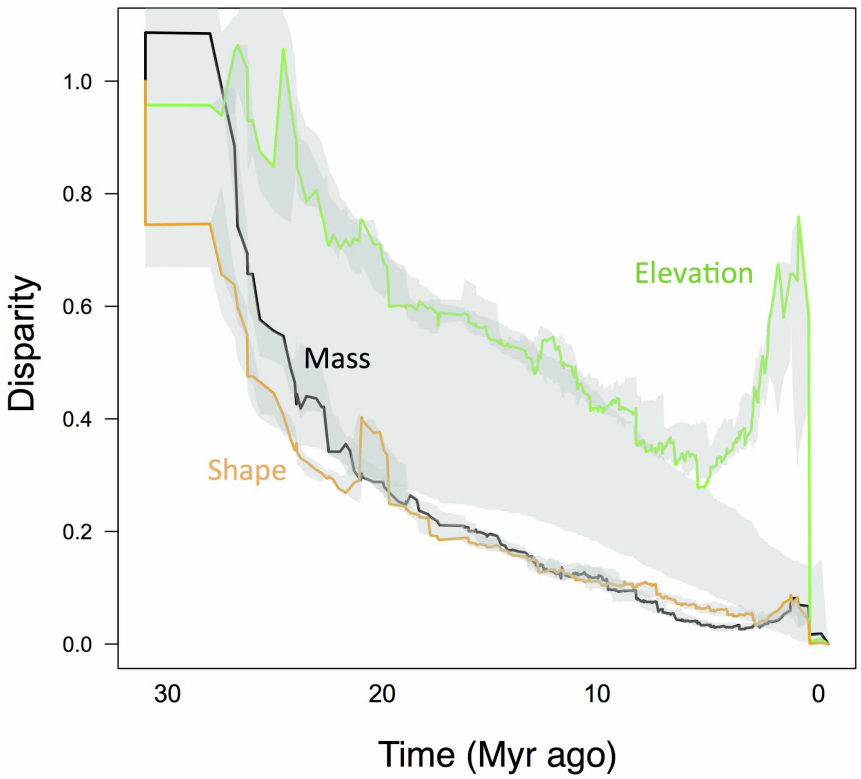

Extended Data Figure 4 | Disparity plots for morphology and habitat, with the null Brownian-motion model added. The large shaded area represents the 95% confidence limit from 100 simulations on 100 trees drawn from the posterior distribution of the Bayesian analysis. The shaded areas around the data plots gives the 95% confidence limits based on phylogenetic uncertainty (based on the same 100 trees as above).

a

Trait	Breakpoint (Ma)	Rate (after/before)
**Log Mass	9 (7.5, 12)	0.3 (0.25, 0.4)
*PC1, Long tarsus, small beak	10 (7.5, 11.5)	0.35 (0.25,0.5)
PC2, Long tarsus, slender beak	14.5 (9, 17.5)	0.5 (0.3, 0.8)

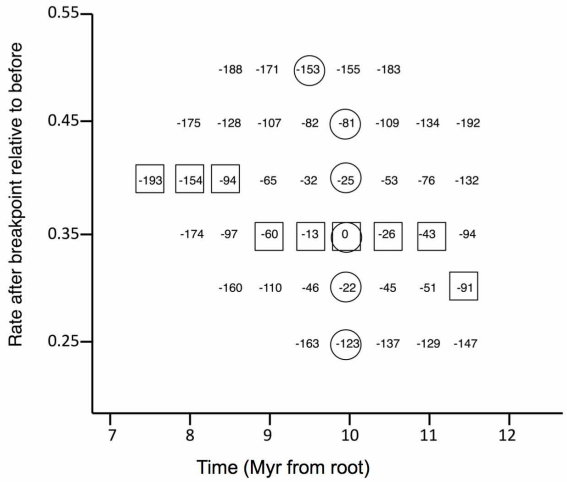

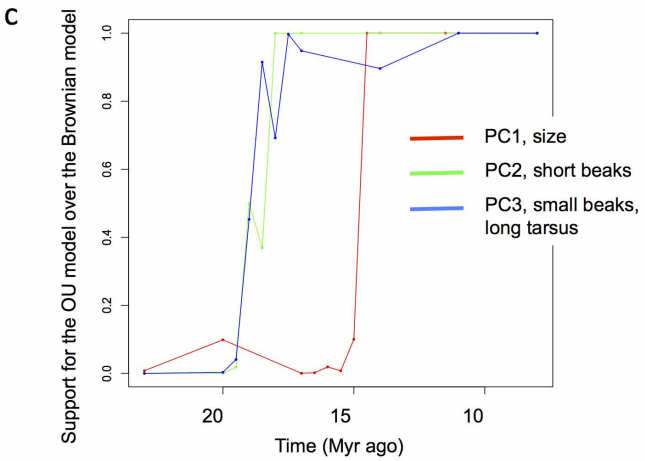

d

Measurement	PC1	PC2	revellPC1	revellPC2	revellPC3
Beak length	-0.2	0.54	0.89	0.16	-0.15
Beak width	-0.59	-0.08	0.92	-0.53	-0.19
Beak depth	-0.51	-0.04	0.95	-0.49	-0.09
Wing length	-0.09	-0.03	0.89	-0.16	0.23
Tarsus length	0.27	0.23	0.71	0.18	0.57

Extended Data Figure 5 | Slowdowns in morphological evolution across the tree of the east Himalayan oscines. **a**, Maximum likelihood breakpoints (the point in time at which one rate becomes favoured over the other) and changes in rate for two-rate models of morphological evolution. Significance values (*$P < 0.01$, **$P < 0.001$) refer to likelihood ratio tests comparing the one- and two-rate Brownian motion models (PC2, $P = 0.16$). 95% support limits (parentheses) were derived from likelihood profiles averaged across 100 trees sampled from the posterior distribution of Bayesian trees. **b**, The likelihood profile for evolution of the first shape index (PC1). The likelihood for each (x, y) combination was obtained as the average across 100 trees, then log-transformed for the figure. Numbers are the difference in log-likelihood from the maximum (×100). Only values less than 2 units are shown. The profiles are indicated by symbols (squares for the breakpoint, and circles for the rate difference). **c**, Relative weights of Ornstein–Uhlenbeck (OU) and Brownian-motion models of morphological evolution at different timelines, based on phylogenetically corrected principal components (revellePCs) (see text). **d**, Correlations of PC scores with the original (log-transformed) variables.

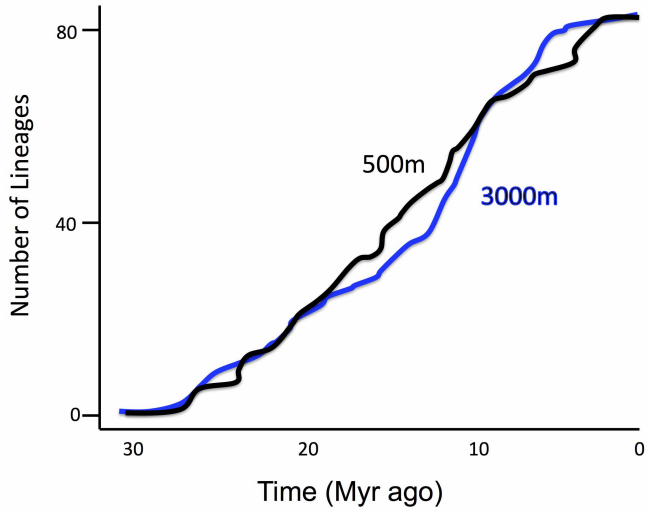

Extended Data Figure 6 | Plot of lineage diversity (on a linear scale) versus time for a phylogeny connecting all species present at 500 m and at 3,000 m. Eighty-two species are estimated to straddle each of these elevational bands.

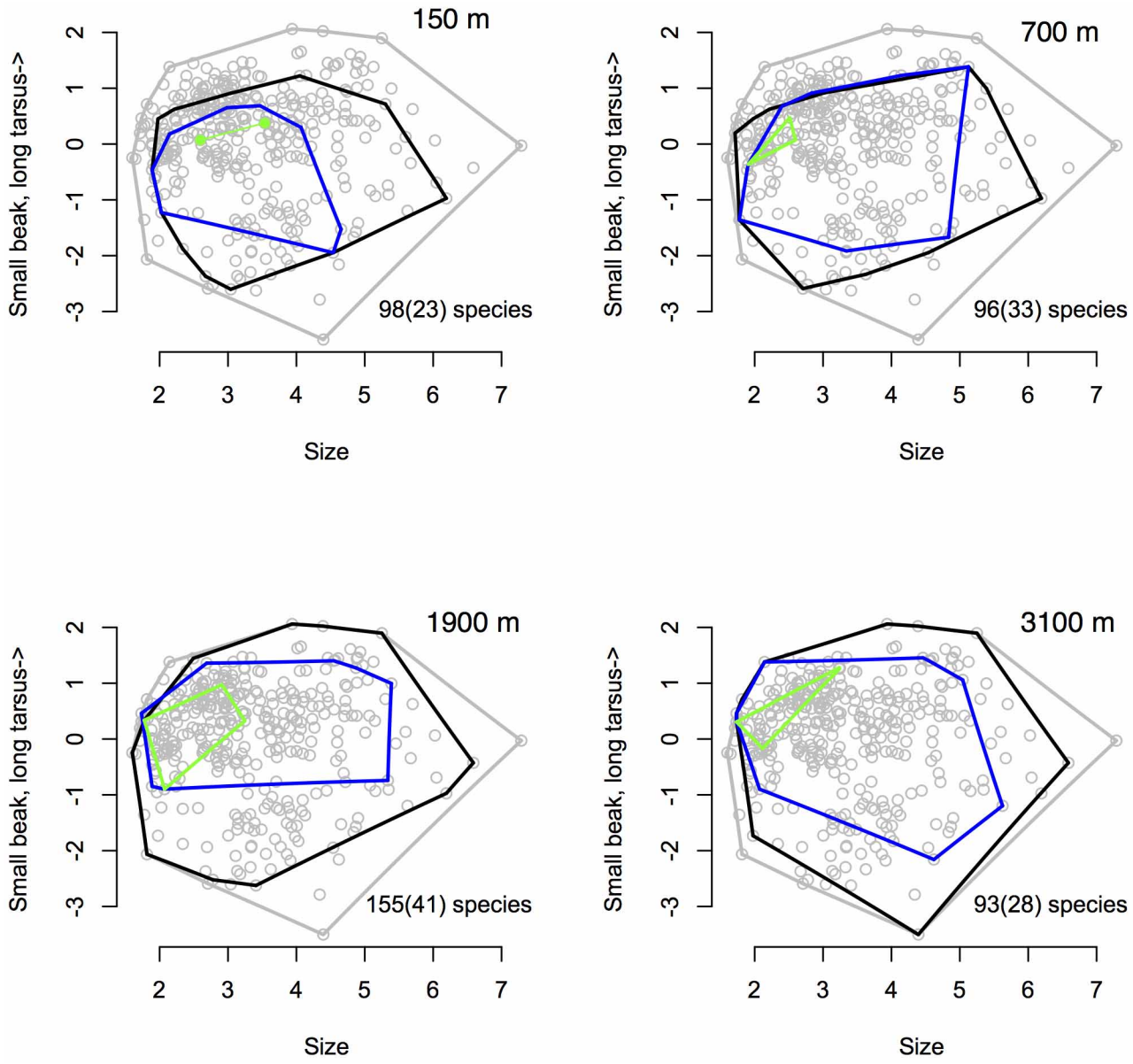

Extended Data Figure 7 | Morphology at specified elevations. Grey lines are the convex hull for all species in the study area (points as in Fig. 2). Black lines are the convex hulls for all species whose elevational ranges include the specified band. Blue lines are the convex hulls for all the species censused on 5-hectare grids at those elevations (see the source data, in order of elevation, B2, A3, B1 and G1), and green lines are the convex hulls for all common (>5 pairs per hectare) species on those grids. Number of species is the number of all bird species in that elevational belt, plus (in parentheses) the number of songbirds censused on the grid.

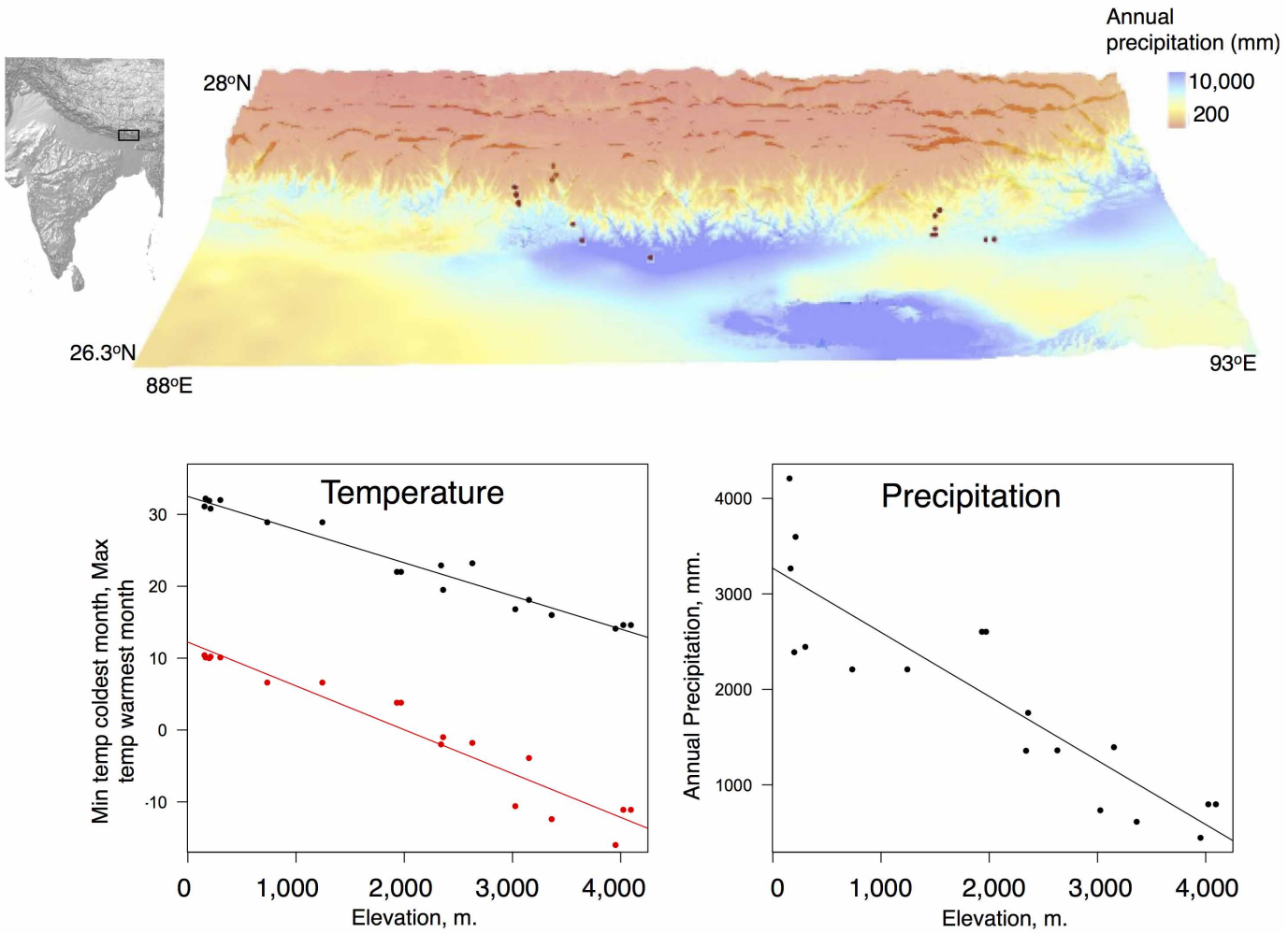

Extended Data Figure 8 | Climate data (from http://worldclim.org33). The top panel shows precipitation mapped on to a topographical map of the study area, showing the locations of the 18 grids. The bottom panels show three predicted climate variables (minimum and maximum temperatures, and precipitation) for the 18 grids. Lines are least-squares regression slopes.

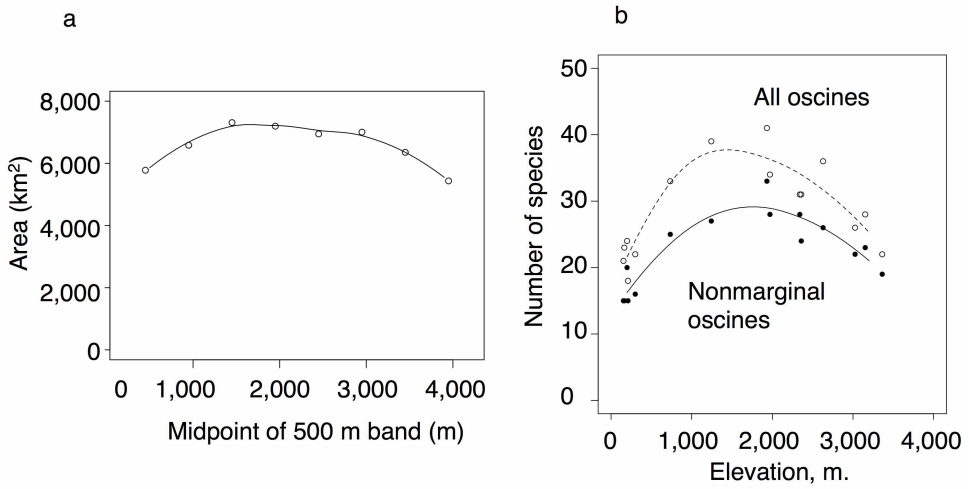

Extended Data Figure 9 | Mid-elevation peak plots. The left panel shows area in 500-m bands between 200 m and 3,700 m in the study area (computed using http://worldclim.org altitude data). The right panel shows the number of oscines in the censused 5-hectare grids and number of oscines in those grids discounted by possible sink species (rare species at the edge of their range).

Extended Data Table 1 | Significance in the downturn in the plot of lineage diversification versus time

Sample space	One tailed P (γ)
*1,504 Asian oscines	P < 0.001 (–2.80)
*1,662 Asian oscines	P < 0.001 (–2.61)
871 tips pure birth model	P < 0.001 (–2.95)
1,546 tips pure birth model	P < 0.001 (–3.12)
7,686 tips pure birth model	P < 0.001 (–3.49)

The significance was assessed by the γ statistic, where a value of less than −1.96 is considered a significant slowdown, when compared to the pure birth (Yule) model[39,43]. The *P* value was assessed by drawing 1,000 random samples of 358 species from the indicated larger phylogenies; the average γ value from the simulations is in parentheses. The asterisk indicates oscines considered to be Asian (from http://avibase.bsc-eoc.org), with relationships described by the tree of ref. 31, including those that Jetz *et al.*[31] inserted without sequence data. The top row is based on the checklist of Clements 2013 and the second row on Clements 2005, as given in the avibase database. Species with different names in the tree of ref. 31 and the Clements compilations were not included ($N = 178$ for 2005, $N = 467$ for 2013). The lower three rows are examples of trees simulated under the Yule model. In all cases the observed γ statistic for the east Himalayan assemblage lay far outside the range of simulated values: The γ statistic for the phylogeny connecting the 358 oscines in the study area based on the tree used here (Fig. 1b) is −13.94 and from the tree of ref. 31 is −8.30 (357 oscines because two *Corvus* were not split in the tree of ref. 31). The γ statistic for a phylogeny truncated at 3 Myr ago is −14.72 (current tree in Fig. 1b, 346 tips), −10.11 (the tree of ref. 31, 330 tips). The time separating sister pairs in the 1,504 Asian species extracted from the Jetz *et al.* tree[31] is 4.0 Myr and the average time of separation of sisters in 358 species samples from that tree 4.5 Myr. For further comparisons with the tree of ref. 31 see the phylogeny construction section in the Methods.